

# Finite size errors in quantum many-body simulations of extended systems

P. R. C. Kent<sup>1</sup>, Randolph Q. Hood<sup>1</sup>, A. J. Williamson<sup>1\*</sup>, R. J. Needs<sup>1</sup>, W. M. C. Foulkes<sup>2</sup>, and G. Rajagopal<sup>1</sup>

<sup>1</sup>*Cavendish Laboratory, Madingley Road, Cambridge CB3 0HE, UK*

<sup>2</sup>*The Blackett Laboratory, Imperial College, Prince Consort Road, London SW7 2BZ, UK*

(June 14, 2021)

Further developments are introduced in the theory of finite size errors in quantum many-body simulations of extended systems using periodic boundary conditions. We show that our recently introduced Model Periodic Coulomb interaction [A. J. Williamson *et al.*, Phys. Rev. B **55**, R4851 (1997)] can be applied consistently to all Coulomb interactions in the system. The Model Periodic Coulomb interaction greatly reduces the finite size errors in quantum many-body simulations. We illustrate the practical application of our techniques with Hartree-Fock and variational and diffusion quantum Monte Carlo calculations for ground and excited state calculations. We demonstrate that the finite size effects in electron promotion and electron addition/subtraction excitation energy calculations are very similar.

PACS: 71.10.-w, 71.15.-m, 71.15.Nc

## I. INTRODUCTION

Most simulations of extended quantum systems are performed using finite simulation cells. This introduces “finite size errors” which are one of the major problems limiting the application of accurate many-body techniques to extended systems. The standard method of reducing the finite size errors is to apply periodic boundary conditions, but important finite size errors often remain. In this paper we present further developments of the theory of finite size effects in quantum many-body simulations subject to periodic boundary conditions. Our motivation is to understand and reduce the finite size effects encountered in quantum Monte Carlo simulations, although the techniques described here are of wide generality and can be readily applied to other many-body electronic structure methods.

Quantum Monte Carlo (QMC) methods in the variational [1] and diffusion [2,3] forms are capable of yielding highly accurate results for correlated electron systems. These methods are very promising because (i) electron correlations are included essentially without approximation and (ii) the methods scale favourably with system size. Nevertheless, for realistic systems the cost of these calculations remains large, and it would be highly desirable to reduce the finite size errors so that accurate results can be obtained using small simulation cells. We stress that all quantum many-body calculations which use periodic boundary conditions to model extended systems suffer from finite size effects and that the ideas discussed in this paper are relevant whenever long ranged interactions are involved.

Finite size errors in many-body calculations have traditionally been corrected for by extrapolation techniques and/or by using the results of more approximate calculations, such as those based on density functional theory (DFT). While extrapolation techniques can certainly be successful they are very costly. In addition, the finite

size errors in periodic boundary condition DFT calculations are significantly different from those in the standard formulations of quantum many-body techniques such as QMC, and therefore a simple application of a DFT finite size correction may not lead to accurate results. We have understood the reason for this difference and have found a way to reduce the finite size errors in quantum many-body simulations using a new “Model Periodic Coulomb” (MPC) interaction, which has the additional advantage that the residual finite size effects are reasonably well described by standard DFT calculations. The accuracy can be further increased by using an extrapolation procedure, but the extrapolation corrections are considerably reduced and can therefore be evaluated using a smaller range of system sizes.

The layout of this paper is as follows. In section II we describe the Hamiltonian within periodic boundary conditions, while in section III we discuss various finite size correction and extrapolation procedures. In section IV we review the “independent particle finite size effects”, showing how our  $k$ -space sampling techniques are related to those used in mean-field theories. In section V we introduce our MPC interaction for reducing finite size effects in periodic systems and show that it can be applied to all the Coulomb interactions. We present tests of the MPC interaction within HF theory (section VIA), VMC (section VIB), and DMC (section VIC). The latter section includes DMC results for a system with 1000 electrons, which is the largest number in any DMC calculation to date. In section VII we discuss finite size errors present in calculations of excitation energies. Tests within HF theory are presented in section VII A, while in section VII B we present VMC results for the “optical absorption” and “photoemission” gaps, the latter being the first such calculations for a three-dimensional periodic system. Calculations with up to 512 electrons demonstrate that the finite size errors in the “optical absorption” and “photoemission” gaps are similar and that

the finite size effects are quite small even for a 64-electron simulation cell. We draw our conclusions in section VIII.

## II. THE HAMILTONIAN WITHIN PERIODIC BOUNDARY CONDITIONS

The many-body Hamiltonian for a system of electrons at positions  $\mathbf{r}_i$  and static ions at positions  $\mathbf{x}_\alpha$  is [4]

$$\hat{H} = \sum_i -\frac{1}{2}\nabla_i^2 + \sum_i \sum_\alpha v_\alpha(\mathbf{r}_i, \mathbf{x}_\alpha) + \frac{1}{2} \sum_i \sum_{j \neq i} v(\mathbf{r}_i, \mathbf{r}_j) + \frac{1}{2} \sum_\alpha \sum_{\beta \neq \alpha} v_{\alpha\beta}(\mathbf{x}_\alpha, \mathbf{x}_\beta) . \quad (1)$$

An infinite system is normally modeled by a finite simulation cell subject to periodic boundary conditions. The model interaction terms,  $v_\alpha$ ,  $v$ , and  $v_{\alpha\beta}$ , are chosen such that the potential energy of the model system, which involves only the positions of the particles in the finite simulation cell, mimics the potential energy of the infinite system as closely as possible. Since the potential energy of the infinite system depends on the positions of all the charges in the solid, only a few of which are included in the simulation, the model interaction energy is approximate even in crystalline solids. To enforce the periodic boundary conditions the functions  $v_\alpha$ ,  $v$ , and  $v_{\alpha\beta}$  must be invariant under the translation of either argument by a member of the set of translation vectors of the simulation cell lattice,  $\{\mathbf{R}\}$ . The standard approach is to choose the model Hamiltonian such that the full potential energy of Eq. 1, evaluated by summing the model interactions between all pairs of particles in the simulation cell, equals the potential energy per cell of an infinite array of identical copies of the simulation cell. However, even when we restrict each simulation cell in the array of copies to be overall charge neutral, the sum of inter-particle Coulomb  $1/r$  interactions is only conditionally convergent, [5] and to define this model interaction uniquely the boundary conditions at infinity must be specified. The standard procedure is to define the potential by solving Poisson's equation subject to periodic boundary conditions, in which case the model interaction is the Ewald interaction. [6] For two electrons separated by  $\mathbf{r}$ , the Ewald interaction is

$$v_E(\mathbf{r}) = \frac{1}{\Omega} \sum_{\{\mathbf{G}\} \neq 0} \frac{4\pi}{G^2} \exp[-G^2/4\kappa^2 + i\mathbf{G} \cdot \mathbf{r}] - \frac{\pi}{\kappa^2 \Omega} + \sum_{\{\mathbf{R}\}} \frac{\text{erfc}(\kappa|\mathbf{r} + \mathbf{R}|)}{|\mathbf{r} + \mathbf{R}|} , \quad (2)$$

where  $\Omega$  is the volume of the simulation cell,  $\{\mathbf{G}\}$  is the set of reciprocal space translation vectors of the simulation cell lattice, and  $\kappa$  is a positive but otherwise arbitrary constant.

## III. FINITE SIZE CORRECTION AND EXTRAPOLATION FORMULAE

The basic idea behind finite size correction formulae is to write the energy for the infinite system as

$$E_\infty = E_N + (E_\infty - E_N) , \quad (3)$$

where the subscript denotes the system size. A highly accurate many-body calculation for the  $N$ -particle system is then performed to obtain an approximation for  $E_N$ , and the correction term in brackets is approximated using a much less expensive scheme which can be applied to very large systems.

In an extrapolation procedure the energy  $E_N$  is calculated for a range of system sizes and fitted to a chosen functional form which contains parameters. Correction and extrapolation procedures can be combined to give an expression

$$E_\infty \simeq E_N + (E'_\infty - E'_N) + F(N) , \quad (4)$$

where the prime indicates that a less expensive scheme is used and  $F(N)$  is an extrapolation function. Clearly, the optimal form of  $F(N)$  depends on the method used to calculate the correction term. The practical difference between correction and extrapolation is that correction requires a single calculation of  $E_N$  using the accurate (and normally very costly) many-body technique, while extrapolation requires several such calculations for different values of  $N$  and a subsequent fit to the chosen functional form  $F(N)$ . The extrapolation procedure is costly because it involves more calculations and is prone to inaccuracy because one has to perform a fit with only a few data points. In designing a correction/extrapolation procedure one therefore tries to make the extrapolation term as small as possible.

Candidate methods for evaluating the correction term include Kohn-Sham DFT and HF theory. The most convenient methods are the local density approximation (LDA) to DFT, or extensions such as the Generalized Gradient Approximation. These methods are very widely applied in periodic boundary conditions calculations and are computationally inexpensive, while retaining a realistic description of the system. Within an independent particle theory, such as Kohn-Sham DFT, calculations for periodic systems are normally performed by solving within the primitive unit cell. [7] To obtain the correct result for the infinite system it is necessary to integrate over  $\mathbf{k}$ -space, and the integral is normally approximated by a sum over a finite set of  $\mathbf{k}$ -points. A determinant formed from the occupied orbitals at a single  $\mathbf{k}$ -point in the first Brillouin zone (BZ) of the primitive unit cell is a many-body wave function for a simulation cell of the size of the primitive unit cell. Adding a second  $\mathbf{k}$ -point doubles the size of the determinant and is equivalent to doubling the size of the simulation cell, etc.

An important subtlety arises when finite size corrections derived from an independent particle theory such as LDA-DFT are used to correct the results of a true many-body method such as QMC. Suppose the many-body calculation is performed using the Ewald interaction, so that the Coulomb energy is that of an infinite periodic array of copies of the simulation cell. Given that the solid we are trying to model is crystalline, and hence the charge density is truly periodic, the Ewald interaction gives a good description of the classical Coulomb or Hartree energy. However, because the electronic positions are mirrored exactly in every copy of the simulation cell, the electronic correlations are also forced to be periodic, and the exchange-correlation (XC) energy corresponds to a system with a periodic XC hole. This unphysical approximation is particularly inaccurate when the simulation cell is small. In Kohn-Sham DFT calculations the XC energy is evaluated using a standard functional such as the LDA of Perdew and Zunger [8], which was obtained by fitting to the results of DMC calculations for jellium. [9] There is an important difference, however, in that the DMC results were extrapolated to the infinite-system-size limit before the fit was made.

The consequences of this difference are nicely illustrated by considering many-body and LDA calculations for jellium, in which the charge density is uniform. The LDA gives the XC energy for the infinite system irrespective of the size of the simulation cell, but the XC energy obtained from a many-body simulation using the Hamiltonian of Eq. 1 with the Ewald interaction gives an XC energy which depends on the size and shape of the simulation cell. Consequently, evaluating the correction term in Eq. 4 within the LDA does not give a good approximation to the finite size correction in the many-body simulation and a significant extrapolation term remains.

The issue of finite size corrections to both the kinetic and interaction energies has been addressed by Ceperley and coworkers. [10–13] Their approach is to add separate extrapolation terms for the kinetic and interaction energies. In their work on hydrogen solids, Ceperley and Alder [11] performed DMC calculations for a number of different system sizes and fitted to the formula

$$E_{\infty}^{\text{DMC}} \simeq E_N^{\text{DMC}} + a(T_{\infty} - T_N) + \frac{b}{N} , \quad (5)$$

where  $a$  and  $b$  are parameters, and  $T$  is the kinetic energy of the non-interacting electron gas. The  $b/N$  term accounts for the finite size effects arising from the interaction energy and the difference of the parameter  $a$  from unity accounts for the difference between the kinetic energies of the interacting and non-interacting systems. Normally  $a > 1$  because the interacting kinetic energy is larger than the non-interacting kinetic energy. Engel *et al.* [14] used the following formula for inhomogeneous systems:

$$E_{\infty}^{\text{QMC}} \simeq E_N^{\text{QMC}} + a(E_{\infty}^{\text{LDA}} - E_N^{\text{LDA}}) + \frac{b}{N} , \quad (6)$$

which reduces to Eq. 5 for a homogeneous system.

As mentioned above, a large part of the finite size error in the interaction energy arises from the use of the Ewald interaction. [15,16] Our approach to the problem of the finite size errors differs from that of Ceperley *et al.* in an important respect. We try to reduce the finite size effects within the *many-body* calculation by modifying the interaction terms in the many-body Hamiltonian. The Ewald interaction is a periodic function which differs from  $1/r$  in such a way that the sum of interactions between pairs of particles *within one cell* gives the exact Coulomb energy per cell of a periodic lattice of identical cells. This ensures that the Ewald Hamiltonian gives the correct Hartree energy, but the deviations from  $1/r$  give rise to a spurious contribution to the XC energy, corresponding to the periodic repetition of the XC hole discussed earlier. [15,16] Our solution is to change the many-body Hamiltonian so that the interaction with the XC hole is exactly  $1/r$  (see section V) for any size and shape of simulation cell, without altering the form of the Hartree energy. This source of finite size error is therefore eliminated and Eq. 3, with the correction term calculated within the LDA, gives a much better description of the remaining finite size errors. Greater accuracy can be obtained by adding an extrapolation term, but this term is much smaller than if the Ewald interaction is used.

The idea of changing the Hamiltonian to reduce the finite size errors may seem strange at first, so it is worth discussing a simple example. Imagine that a periodic boundary condition QMC technique is being used to study an isolated molecule. If the molecule is placed at the center of the periodically repeated simulation cell, the calculated energy is that of an array of identical molecules, including unwanted inter-molecular interactions. The results improve as the simulation cell is made larger, but the convergence is slow, especially for molecules with permanent dipole moments. A better solution is to cut off all Coulomb interactions between charges on different molecules, i.e., to replace the Ewald interactions by truncated Coulomb  $1/r$  interactions acting only within the simulation cell. As long as the molecular wave function has decayed to zero before the simulation cell boundary is reached, this procedure should give essentially exact results. The changes to the interaction to be discussed in this paper are a generalization of this approach to make it useful in simulating genuinely periodic systems such as crystals. In this case the very “strict” notion of periodicity built into the Ewald interaction produces an artificial periodic replication of the XC hole as well as the required periodic replication of the charge density. Our modified Hamiltonian removes the effects of the unwanted extra periodicity just as the simple truncation removed the unwanted periodicity in the molecular example.

An alternative procedure is to evaluate the correction term in Eq. 3 using HF data. HF theory is an approximate method for solving the many-body Hamiltonian, and if we use the Ewald formula for the electron-electron interaction terms in both the many-body and HF theories, the finite size error in the HF exchange energy will tend to cancel the finite size error in the many-body interaction energy. At first sight this appears to be an excellent solution to the finite size problem. However, this procedure gives too large a correction, presumably because the HF exchange hole is significantly different from the screened XC hole of the many-body system.

#### IV. INDEPENDENT PARTICLE FINITE SIZE EFFECTS

We call the correction term  $(E_{\infty}^{\text{LDA}} - E_N^{\text{LDA}})$  the “independent particle finite size effect” (IPFSE). The finite size effect arising from the particular model interaction used is called the “Coulomb finite size effect” (CFSE). In this section we discuss the IPFSE in more detail. The “finite size error” in an LDA calculation for a perfect crystal arises from errors in the BZ integration. In an LDA calculation the computational cost is proportional to the number of k-points used. However, in a QMC calculation the volume of the simulation cell is proportional to the number of k-points in the primitive BZ and the computational cost increases approximately as the cube of the volume of the simulation cell. This means that it is even more important to choose the k-points carefully in a QMC calculation so as to make the IPFSE as small as possible.

Additional errors arise when using the supercell approximation for systems which break translational symmetry. Consider a crystal containing a point defect. In the supercell approach a finite simulation cell containing a single defect is repeated throughout space to form an infinite three-dimensional array. The supercell must be sufficiently large that the interaction between defects in different cells is negligible. This type of finite size effect is distinct from the BZ integration error because it persists even when the BZ integration is performed exactly. However, the correction to the defect formation energy from this type of finite size error should be described reasonably well by a  $(E_{\infty}^{\text{LDA}} - E_N^{\text{LDA}})$  correction term, where  $E_{\infty}^{\text{LDA}}$  and  $E_N^{\text{LDA}}$  are, respectively, the defect formation energies for a large simulation cell and a smaller one, each containing a single defect.

A determinantal Bloch wave function suitable for use in a QMC calculation may be formed from a set of single particle orbitals at a single k-point,  $\mathbf{k}_s$ , in the Brillouin zone of the simulation cell reciprocal lattice. The IPFSE can be greatly reduced for insulating systems by a careful choice of  $\mathbf{k}_s$  using the method of “special k-points” borrowed from band structure theory. [17,18] We

have described the theory of the “special k-points” for many-body calculations in our earlier work [19,20] and here we concentrate on the practicalities of choosing  $\mathbf{k}_s$ . Baldereschi [17] defined the “mean-value point”, which is a k-point at which smooth periodic functions of wave vector accurately approximate their averages over the BZ, and clearly the Baldereschi mean-value point is a strong candidate for  $\mathbf{k}_s$ . However, we find it convenient to choose  $\mathbf{k}_s$  to be equal to half a translation vector of the simulation cell reciprocal lattice ( $\mathbf{k}_s = \mathbf{G}/2$ ), which allows the construction of real single-particle orbitals and hence is computationally more efficient. Some freedom is still left in the selection of  $\mathbf{k}_s$ , and we choose from the  $\mathbf{G}/2$  according to the symmetrized plane wave test of BZ integration quality introduced by Baldereschi. [17] For example, for an fcc simulation cell the half-reciprocal-lattice vectors correspond to the  $\Gamma$ ,  $X$  and  $L$  points of the BZ of the simulation cell reciprocal lattice. For a crystal with the full cubic symmetry  $\mathbf{k}_s \equiv L$  gives the best BZ integration and  $\mathbf{k}_s \equiv \Gamma$  the worst.

It is illuminating to relate these k-point schemes to the multi-point schemes used in LDA and HF calculations. In LDA and HF calculations one normally samples the BZ of the primitive unit cell, whereas in a QMC calculation one samples the BZ of the simulation cell. Suppose that the simulation cell has translation vectors  $N_1\mathbf{a}_1$ ,  $N_2\mathbf{a}_2$ , and  $N_3\mathbf{a}_3$ , where the  $N_i$  are integers and the  $\mathbf{a}_i$  are vectors defining the primitive unit cell. When unfolded into the BZ of the primitive unit cell the k-point  $\mathbf{k}_s$  maps onto the regular mesh

$$\mathbf{k}_{lmn} = \frac{l}{N_1}\mathbf{b}_1 + \frac{m}{N_2}\mathbf{b}_2 + \frac{n}{N_3}\mathbf{b}_3 + \mathbf{k}_s, \quad (7)$$

where  $l = 0, \dots, N_1 - 1$ ,  $m = 0, \dots, N_2 - 1$ ,  $n = 0, \dots, N_3 - 1$ , and the  $\mathbf{b}_i$  are reciprocal to the  $\mathbf{a}_i$ . This mesh is of the same type as defined in the widely-used Monkhorst-Pack scheme [18] for BZ integration, differing only by an offset from the origin. The multi-point generalization of the Baldereschi scheme which can be used in LDA and HF calculations is now obvious: one chooses the offset  $\mathbf{k}_s$  to be equal to the mean-value point [17] of the lattice defined by the translation vectors  $N_i\mathbf{a}_i$ . As mentioned above, for our purposes we prefer to choose  $\mathbf{k}_s$  to be equal to half a translation vector of the simulation cell reciprocal lattice. This choice gives a smooth and rapid convergence of the BZ integration with increasing values of the  $N_i$  [20]. For example, as mentioned above, for fcc crystals we choose  $\mathbf{k}_s$  to be an  $L$ -point of the BZ of the lattice defined by the  $N_i\mathbf{a}_i$ . In this case the Monkhorst-Pack [18] definition of the offset corresponds to taking an  $L$ -point for  $N_i$  even, but the  $\Gamma$ -point for  $N_i$  odd. The latter choice gives poor results and this problem has prompted some researchers to avoid Monkhorst-Pack meshes with odd values of the  $N_i$ , but in fact odd values can be very efficient if the mesh is offset according to our prescription.

## V. COULOMB FINITE SIZE EFFECTS

In this section we summarize the theory of the MPC interaction. More details and background are given in Refs. [15] and [16]. In section III we described how the CFSE arises from the XC energy and the dependence of the Ewald interaction,  $v_E$ , on the size and shape of the simulation cell. Expanding  $v_E$  around zero separation gives [15,16]

$$v_E(\mathbf{r}) = \text{constant} + \frac{1}{r} + \frac{2\pi}{3\Omega} \mathbf{r}^T \cdot \mathbf{D} \cdot \mathbf{r} + \mathcal{O}\left(\frac{r^4}{\Omega^{5/3}}\right), \quad (8)$$

where  $\Omega$  is the volume of the simulation cell, and the tensor  $\mathbf{D}$  depends on the shape of the simulation cell. (For a cubic cell  $\mathbf{D}=\mathbf{I}$ .) The constant term arises from the condition that the average of  $v_E$  over the simulation cell is zero. The term of order  $r^2$  and the higher order deviations from  $1/r$  make the Ewald interaction periodic and ensure that the sum of interactions between the particles in the simulation cell gives the potential energy per cell of an infinite periodic lattice. These terms are responsible for the spurious contribution to the XC energy, which is the source of the large finite size effect in many-body calculations using the Ewald interaction. [15,16] For cubic cells the interaction at short distances is larger than  $1/r$  and therefore the XC energy is more negative than it should be, and because the leading order correction is proportional to the inverse of the simulation cell volume the error per electron is inversely proportional to the number of electrons in the cell.

Clearly it is desirable to remove this spurious contribution to the XC energy, but we must remember that the Hartree energy is correctly evaluated using the Ewald interaction. The key requirements for a model Coulomb interaction giving small CFSEs in simulations with periodic boundary conditions are therefore: (i) it should give the Ewald interaction for the Hartree terms, and (ii) it should be exactly  $1/r$  for the interaction with the XC hole. Unfortunately, the only periodic solution of Poisson's equation for a periodic array of charges is the Ewald interaction, which obeys criterion (ii) only in the limit of an infinitely large simulation cell. We therefore abandon the use of Poisson's equation and the Ewald interaction, and instead use a "Model Periodic Coulomb" (MPC) interaction which satisfies both criteria. This may seem a drastic step, but we point out that we are trying to model an infinite system by a finite one and that the inter-particle interaction used in the finite simulation cell must model the effects of all the charges in the infinite system.

Our MPC interaction [16] can be written as

$$\begin{aligned} \hat{H}_{e-e} = & \sum_{i>j} f(\mathbf{r}_i - \mathbf{r}_j) \\ & + \sum_i \int_{\text{WS}} [v_E(\mathbf{r}_i - \mathbf{r}) - f(\mathbf{r}_i - \mathbf{r})] \rho(\mathbf{r}) d\mathbf{r}, \end{aligned} \quad (9)$$

where  $\rho$  is the electronic charge density and

$$f(\mathbf{r}) = \frac{1}{r_m}. \quad (10)$$

The definition of the cutoff Coulomb function,  $f$ , involves a minimum image convention whereby the inter-electron distance,  $\mathbf{r}$ , is reduced into the Wigner-Seitz (WS) cell of the simulation cell lattice by removal of simulation cell lattice translation vectors, leaving a vector  $\mathbf{r}_m$ . This ensures that  $\hat{H}_{e-e}$  has the correct translational and point group symmetry. The first term in Eq. 9 is a direct Coulomb interaction between electrons within the simulation cell and the second term is a sum of potentials due to electrons "outside the simulation cell". Note that the second term is a one-body potential similar to the Hartree potential. It depends on the electronic charge density,  $\rho$ , but is not a function of the separation of the electrons.

The electron-electron contribution to the total energy is evaluated as the expectation value of  $\hat{H}_{e-e}$  with the many-electron wave function,  $\phi$ , minus a double counting term:

$$\begin{aligned} E_{e-e} = & \langle \phi | \hat{H}_{e-e} | \phi \rangle \\ & - \frac{1}{2} \int_{\text{WS}} \rho(\mathbf{r}) \rho(\mathbf{r}') [v_E(\mathbf{r} - \mathbf{r}') - f(\mathbf{r} - \mathbf{r}')] d\mathbf{r} d\mathbf{r}'. \end{aligned} \quad (11)$$

Evaluating the expectation value gives

$$\begin{aligned} E_{e-e} = & \frac{1}{2} \int_{\text{WS}} \rho(\mathbf{r}) \rho(\mathbf{r}') v_E(\mathbf{r} - \mathbf{r}') d\mathbf{r} d\mathbf{r}' \\ & + \left( \int_{\text{WS}} |\phi|^2 \sum_{i>j} f(\mathbf{r}_i - \mathbf{r}_j) \Pi_k d\mathbf{r}_k \right. \\ & \left. - \frac{1}{2} \int_{\text{WS}} \rho(\mathbf{r}) \rho(\mathbf{r}') f(\mathbf{r} - \mathbf{r}') d\mathbf{r} d\mathbf{r}' \right), \end{aligned} \quad (12)$$

where the first term on the right hand side is the Hartree energy and the term in brackets is the XC energy. We can see immediately that the Hartree energy is calculated with the Ewald interaction while the XC energy (expressed as the difference between a full Coulomb term and a Hartree term) is calculated with the cutoff interaction  $f$ .

The charge density  $\rho$  appears in Eqs. 9, 11, and 12. In QMC methods, the charge density is known with greatest statistical accuracy at the end of the calculation. This is not a serious complication for VMC simulations as the interaction energy may be evaluated at the end of the simulation using the accumulated charge density. In DMC this is not possible because the local energy [2,3] is required at every step. We investigate this point further in section VIC.

The CFSE may be viewed in another way [15]. Consider a large cluster of identical simulation cells. Almost all possible configurations of the electrons within the

simulation cell have a net dipole moment. The dipole moments in the periodic replicas of the simulation cell are aligned, resulting in a depolarization field across the sample. (In real non-ferroelectric solids the dipoles from different regions are not aligned and the depolarization field is greatly reduced.) To make the electrostatic potential periodic deep within the cluster we need to apply a cancelling external electric field. In the limit of a very large cluster this is equivalent to using the Ewald interaction. In a cubic system the total energy of interaction between the dipoles, which includes the interaction with the depolarization field, does not contribute to the  $\mathcal{O}(r^2)$  term in Eq. 8 [21]. For a cubic system the  $\mathcal{O}(r^2)$  term in Eq. 8 therefore arises solely from the interaction between the dipoles and the external field. In a non-cubic system the  $\mathcal{O}(r^2)$  term contains contributions from both the dipole-dipole interactions and the interactions of the dipoles with the external field. The advantage of our MPC interaction is that it prevents the  $\mathcal{O}(r^2)$  terms contributing to the XC energy.

If the simulation cell is not big enough to accommodate the true XC hole then the XC hole is squeezed into the cell and a finite size error ensues. This appears to be the largest finite size error in the interaction energy after the CFSE has been removed. Extrapolation currently appears to be the best method of correcting this error. When the XC hole is squeezed by the finite simulation cell the XC energy calculated using the MPC interaction is too negative. The effect of the  $\mathcal{O}(r^2)$  term in the Ewald interaction is to make it even more negative, however, and so the MPC interaction is still better than the Ewald interaction.

### A. Systems of electrons and nuclei

In the previous sections we considered the electron-electron interaction only, and did not discuss the electron-nucleus and nucleus-nucleus interactions. If the MPC interaction is physically reasonable we should, however, be able to apply it to all the interactions in the problem, not just the electron-electron terms. Here we apply the MPC interaction to a system of electrons and nuclei, showing that under certain common conditions the expressions simplify so that the electron-nucleus and nucleus-nucleus terms reduce to the Ewald form.

Consider a simulation cell with periodic boundary conditions containing  $N$  electrons at positions  $\mathbf{r}_i$  and  $M$  nuclei of charge  $Z_\alpha$  at positions  $\mathbf{x}_\alpha$ . The wave function of the electrons and nuclei is  $\Psi(\{\mathbf{r}_i\}, \{\mathbf{x}_\alpha\})$ , and the total charge density (electrons and nuclei) is  $\rho_T(\mathbf{r})$ . The interaction energy calculated with the MPC interaction is

$$E_{\text{int}} = \frac{1}{2} \int_{\text{WS}} \rho_T(\mathbf{r}) \rho_T(\mathbf{r}') [v_E(\mathbf{r} - \mathbf{r}') - f(\mathbf{r} - \mathbf{r}')] d\mathbf{r} d\mathbf{r}'$$

$$+ \int_{\text{WS}} |\Psi|^2 \left[ \sum_{i>j} f(\mathbf{r}_i - \mathbf{r}_j) - \sum_i \sum_\alpha Z_\alpha f(\mathbf{r}_i - \mathbf{x}_\alpha) + \sum_{\alpha>\beta} Z_\alpha Z_\beta f(\mathbf{x}_\alpha - \mathbf{x}_\beta) \right] \Pi_k d\mathbf{r}_k \Pi_\gamma d\mathbf{x}_\gamma \quad (13)$$

We now employ the adiabatic approximation to separate the electronic and nuclear dynamical variables:

$$\Psi(\{\mathbf{r}_i\}, \{\mathbf{x}_\alpha\}) = \phi(\{\mathbf{r}_i\}; \{\mathbf{x}_\alpha\}) \Phi(\{\mathbf{x}_\alpha\}) \quad (14)$$

where the  $\{\mathbf{x}_\alpha\}$  appear only as parameters in  $\phi$ . To make further progress we must assume a form for the nuclear part of the wave function,  $\Phi$ . The simplest assumption is that  $\Phi$  can be written as an appropriately symmetrized product of very strongly localized non-overlapping single-nucleus functions. Regardless of whether the product is antisymmetrized, symmetrized, or not symmetrized, Eq. 13 reduces to

$$E_{\text{int}} = \frac{1}{2} \int_{\text{WS}} \rho(\mathbf{r}) \rho(\mathbf{r}') [v_E(\mathbf{r} - \mathbf{r}') - f(\mathbf{r} - \mathbf{r}')] d\mathbf{r} d\mathbf{r}' + \int_{\text{WS}} |\phi|^2 \sum_{i>j} f(\mathbf{r}_i - \mathbf{r}_j) \Pi_k d\mathbf{r}_k - \int_{\text{WS}} |\phi|^2 \sum_i \sum_\alpha Z_\alpha v_E(\mathbf{r}_i - \bar{\mathbf{x}}_\alpha) \Pi_k d\mathbf{r}_k + \sum_{\alpha>\beta} Z_\alpha Z_\beta v_E(\bar{\mathbf{x}}_\alpha - \bar{\mathbf{x}}_\beta) \quad (15)$$

where the  $\bar{\mathbf{x}}_\alpha$  denote the centers of the single-nucleus functions and  $\rho$  is the electron density. Note that the electron-nucleus and nucleus-nucleus terms involve only the Ewald interaction and that the first two terms of Eq. 15 correspond precisely to the electron-electron interaction of Eq. 12. This result justifies the use of Eq. 9 for the electron-electron interactions while retaining the Ewald interaction for the electron-nucleus and nucleus-nucleus terms.

## VI. TESTS OF THE MPC INTERACTION

### A. Application to HF calculations

We have tested the MPC interaction by performing a series of calculations on diamond structure silicon using fcc simulation cells whose translation vectors are  $n$  times those of the primitive unit cell. In a previous publication we gave a few results from such tests [16], but here we present new tests and subject them to a more detailed analysis.

In our first set of tests we compare LDA and HF results. These tests are inexpensive, which allows us to study very large systems, and they are not subject to

statistical errors because Monte Carlo techniques are not involved. We consider simulation cells with  $n = 1, 2, 3, 4$ , and  $5$ , which contain  $2, 16, 54, 128$ , and  $250$  ions, respectively. The  $\text{Si}^{4+}$  ions were represented by norm-conserving non-local LDA pseudopotentials and the calculations were performed using a plane-wave basis set with a cutoff energy of  $15$  Ry. To facilitate comparison we evaluate the HF energy with the LDA orbitals, so that the energy differences arise solely from the difference between the LDA XC energy and the HF exchange energy. We performed calculations using  $\mathbf{k}_s \equiv L$  and  $\mathbf{k}_s \equiv \Gamma$ . The HF energy evaluated with the MPC interaction is

$$\begin{aligned}
E^{\text{HF}} = & \sum_i -\frac{1}{2} \int \phi_i^*(\mathbf{r}) \nabla^2 \phi_i(\mathbf{r}) d\mathbf{r} \\
& + \frac{1}{2} \int \rho(\mathbf{r}) \rho(\mathbf{r}') v_E(\mathbf{r} - \mathbf{r}') d\mathbf{r} d\mathbf{r}' \\
& - \frac{1}{2} \sum_{i,j}^N \delta_{s_i s_j} \int \phi_i^*(\mathbf{r}) \phi_i(\mathbf{r}') f(\mathbf{r} - \mathbf{r}') \phi_j^*(\mathbf{r}') \phi_j(\mathbf{r}) d\mathbf{r} d\mathbf{r}' \\
& + \int V_{\text{ext}}(\mathbf{r}) \rho(\mathbf{r}) d\mathbf{r} + E_{\text{I-I}} \quad , \quad (16)
\end{aligned}$$

where  $E_{\text{I-I}}$  is the ion-ion energy calculated with the Ewald interaction. Note that the Hartree energy is evaluated with the Ewald interaction while the exchange energy is evaluated with the cutoff Coulomb interaction.

In Fig. 1 we show the deviations of the LDA and HF energies from the fully converged values as a function of system size for  $\mathbf{k}_s \equiv \Gamma$  wave functions. The LDA energy converges smoothly with system size but for small system sizes the IPFSE error is large because of the  $\Gamma$ -point sampling. We show HF energies calculated with the Ewald and MPC interactions, with and without incorporating the IPFSE corrections obtained from the LDA data. The data incorporating the IPFSE (filled symbols) show the residual CFSE errors. The IPFSE is positive while the CFSE is negative, in accord with the analysis of the CFSE given in section V. The IPFSE corrected data show that the CFSE for the MPC interaction is roughly half that for the Ewald interaction.

In Fig. 2 we show similar data for  $\mathbf{k}_s \equiv L$ . The LDA energy converges rapidly and smoothly with system size, and therefore the IPFSE is small, which demonstrates the efficacy of the “special k-points” method. The IPFSE and CFSE errors tend to cancel and for  $\mathbf{k}_s \equiv L$  sampling the HF data converge more rapidly without the IPFSE corrections. For  $n = 3$ , corresponding to a  $54$  atom simulation cell, the LDA finite size error (IPFSE only) is  $0.011$  eV per atom, which is very much smaller than the HF (Ewald) finite size error of  $-0.211$  eV per atom or the equivalent HF (MPC) error of  $-0.071$  eV per atom. As in the case of  $\Gamma$ -point sampling, the CFSE for the MPC interaction is roughly half that for the Ewald interaction.

After applying the IPFSE correction obtained from the LDA data the HF results for  $\mathbf{k}_s \equiv \Gamma$  and  $\mathbf{k}_s \equiv L$  sampling

are very similar. The correspondence of the IPFSE corrected data for the  $L$ - and  $\Gamma$ -points demonstrates that to a very good approximation the IPFSE and CFSE are independent. Estimating the energy of the infinite system by averaging the energy over a set of  $\mathbf{k}_s$  vectors removes the IPFSE but does not remove the CFSE.

We have fitted the CFSE errors from the filled data points in Figs. 1 and 2 to the form  $b/N^x$ , where  $b$  and  $x$  are parameters and  $N = 8n^3$  is the number of electrons in the simulation cell. The fits give values of  $x$  in the region of unity for both the Ewald and MPC interactions. This extrapolation function is therefore suitable for both interactions, although the size of the extrapolation term is smaller for the MPC interaction.

The Ewald and MPC interactions differ by an amount inversely proportional to the volume of the simulation cell. This means that although the energies per particle converge to the same value as the volume of the simulation cell increases, the difference between the Ewald and MPC energies of the whole simulation cell tends to a finite constant as the simulation cell volume goes to infinity. We have evaluated this constant value for the fixed-LDA-orbital HF calculations described in this section by extrapolating the energy difference between the Ewald and MPC energies. This gives a value of approximately  $14$  eV.

## B. Application to VMC

In the VMC method [1,3] the energy is calculated as the expectation value of the Hamiltonian,  $\hat{H}$ , with a trial wave function,  $\phi_T$ , yielding a rigorous upper bound to the exact ground state energy. The Metropolis algorithm is used to generate electron configurations distributed according to  $\phi_T^2$ , and the energy calculation is performed by averaging the local energy,  $\phi_T^{-1} \hat{H} \phi_T$ , over this distribution.

Our trial wave functions are of the standard Slater-Jastrow type:

$$\phi_T = D^\uparrow D^\downarrow \exp \left[ \sum_{i=1}^N \chi(\mathbf{r}_i) - \sum_{i<j}^N u(r_{ij}) \right] \quad , \quad (17)$$

where there are  $N$  electrons in the simulation cell,  $\chi$  is a one-body function,  $u$  is a two-body correlation factor which depends on the relative spins of the two electrons, and  $D^\uparrow$  and  $D^\downarrow$  are Slater determinants of up- and down-spin single-particle orbitals. The  $u$  functions were of the type described in [22], while for the  $\chi$  functions we used spherically symmetric functions centered on each atom. These  $\chi$  functions give significantly better results than the truncated Fourier series representation used in our earlier work. [22,16] The trial wave functions contained  $32$  variable parameters, whose optimal values were obtained by minimizing the variance of the energy using

10,000–20,000 statistically independent electron configurations, which were regenerated several times during the minimization procedure. [22,23] We used the same pseudopotential as in our LDA and HF calculations, sampling the non-local potential using the techniques of Fahy *et al.* [24].

We have optimized wave functions using both the Ewald and MPC interactions. The wave functions generated using the different interactions are almost identical. Properties other than the energy, such as pair correlation functions, are therefore hardly affected by the choice of interaction. As the MPC interaction gives the correct interaction between the electrons at short distances it may give a better account of, for example, the short distance behaviour of the pair correlation function, but more numerical work is required to investigate this point.

In Fig. 3 we show results for VMC calculations of the energies of the same systems as in the previous section. These results are similar to those given in Ref. [16], but they have been recalculated for this work with more accurate wave functions and better sampling, and the data have been corrected for the IPFSE. The total energies were calculated to a statistical accuracy of  $\pm 0.01$  eV per atom. The VMC data display a smaller CFSE than the HF data, probably because the HF exchange hole is longer ranged than the screened hole obtained in the correlated calculations. For  $n = 2$ , the MPC interaction reduces the VMC finite size error by more than 50%, from  $-0.403$  to  $-0.187$  eV per atom.

### C. Application to DMC

In the DMC method [2,3], imaginary time evolution of the Schrödinger equation is used to evolve an ensemble of  $3N$ -dimensional electronic configurations towards the ground state. The calculations are made tractable by using the fixed node approximation and by incorporating importance sampling. The method generates the distribution  $\phi_T \psi$ , where  $\psi$  is the best (lowest energy) wave function with the same nodes as the guiding wave function,  $\phi_T$ . The accuracy of the fixed node approximation can be tested on small systems and the results are normally very satisfactory. [3]

We evaluated the non-local pseudopotential energy using the “locality approximation”. [25] The short-time approximation for the Green’s function was used with a time step of 0.01 a.u. Li *et al.* [26] found that using a time step of 0.015 a.u. gave a time-step error of less than 0.03 eV per atom in silicon, so our time step error should be even smaller. The total energies were calculated to a statistical accuracy of  $\pm 0.02$  eV per atom.

Our MPC interaction is more complicated to apply in DMC than in VMC because the evaluation of the importance sampled Green’s function requires the local energy. The modified Hamiltonian, and hence the local

energy, depends on the charge density, and therefore we must know the charge density before we can perform the DMC calculation. Fortunately, however, the local energy is relatively insensitive to the charge density used in the Hamiltonian (Eq. 9) because  $v_E(\mathbf{r}) - f(\mathbf{r})$  is small when  $|\mathbf{r}|$  is small.

We have tested the sensitivity of the Green’s function to the charge density used in the Hamiltonian. Two candidate charge densities are the charge density of the determinantal part of the QMC wave function and the charge density of the VMC guiding wave function. Even for a small system ( $n = 2$ ) we find it sufficient to use the LDA charge density during the calculation of the Green’s function and to re-evaluate the charge density dependent term in the interaction energy using the DMC density obtained at the end of the calculation. The sensitivity rapidly reduces with increasing system size, and this procedure gives errors of less than 0.03 eV per atom for  $n = 2$ , and less than 0.01 eV per atom for larger system sizes. Therefore, the requirement of having a good approximation to the charge density in advance of the DMC calculation does not pose a significant difficulty. A successful DMC calculation requires a good quality VMC trial function and its charge density can be obtained during the process of wave function optimization.

In Fig. 4 we show results for DMC calculations on the same systems as for our VMC study, the largest of which contains 1000 electrons. The results include a correction for the IPFSE. The convergence behaviour is very similar to the VMC data. The MPC energies are always above those for the Ewald interaction and the MPC interaction significantly reduces the CFSE. These results demonstrate that the finite size errors within VMC and DMC calculations are very similar and that the MPC interaction is similarly effective in both methods.

We have fitted the residual CFSE errors in both the VMC and DMC calculations to the form  $b/N^x$ . The fit is reasonable and gives a value of  $x$  close to unity for both the Ewald and MPC data. For these data it is possible to obtain more accurate approximations to  $E_{\infty}^{\text{QMC}}$  by using such an extrapolation function, although the calculations for the large system sizes are costly, especially within DMC. The extrapolated energies should be more accurate for the MPC interaction because the extrapolation term is significantly smaller.

Many interesting applications of VMC and DMC methods will be to problems in which the quantity of physical interest is the difference in energy between two large systems. Examples of such problems are calculations of excitation energies and defect energies in solids. In such cases the energy of interest is approximately independent of the size of the simulation cell, so that for each simulation cell size it is the energy of the *whole simulation cell* which must be converged to the required tolerance, not the energy per atom as we plotted in Figs. 3 and 4. In these cases extrapolation will be so costly that it can



hardly be contemplated. In some cases the CFSE will largely cancel between the two systems, as occurs in our excitation energy calculations (see next section). This cancellation cannot always be relied upon, however, especially when the simulation cells contain different numbers of particles, and the use of the MPC interaction should be particularly beneficial in such cases.

## VII. EXCITATION ENERGIES

The quasiparticle excitation energies are the energies for adding an electron to the system or subtracting one from it. A quasiparticle energy has both real and imaginary parts, the latter giving the quasiparticle lifetime. For the minimum energy electron and hole quasiparticle excitations the imaginary parts of the quasiparticle energies are zero and the quasiparticles have an infinite lifetime. In this case the exact quasiparticle energy gap can be written as

$$E_g = (E_{N+1} - E_N) + (E_{N-1} - E_N), \quad (18)$$

where  $E_{N+1}$ ,  $E_{N-1}$ , and  $E_N$  are the ground state total energies of the  $N + 1$ ,  $N - 1$  and  $N$  electron systems. A general quasiparticle energy gap cannot be written in terms of differences between energies of exact eigenstates of the system, but such an approximation is often accurate for low energy gaps. The quasiparticle energies are measured in photoemission and inverse photoemission experiments. In an optical absorption experiment a different process occurs in which an electron is excited from the valence to the conduction band. This introduces two quasiparticles into the system, the electron and hole, which interact and can form an exciton, in which case the lowest excitation energy is smaller than  $E_g$  by the exciton binding energy,  $E_b$ .

The HF method gives approximations to the energies of quasiparticles and the interactions between them. According to Koopmans' theorem, if orbital relaxation is neglected, the quasiparticle energies are equal to the HF eigenvalues. Koopmans' theorem can be extended to include correlation effects. [27,28] The extended Koopmans' theorem has been used in conjunction with VMC methods to calculate quasiparticle energies in silicon. [29] In both of these methods the "quasiparticle energies" are real as they are obtained as approximations to the energy differences between exact eigenstates of the system.

Recently there has been significant progress in applying QMC techniques to calculate approximate excitation energies from eigenstates using "direct methods". In these approaches an excitation energy is obtained by performing separate QMC calculations for the ground and excited states. A Slater-Jastrow wave function is used for the ground state, and for the optical gap the excited state is formed by replacing a valence band single

particle orbital by a conduction band one. We call this a "promotion" calculation, and such calculations have been reported for a nitrogen solid [30], diamond [31,32], and silicon [33]. Photoemission/inverse photoemission gaps may be obtained by using QMC to calculate the ground state energies of the  $N + 1$ ,  $N - 1$ , and  $N$  electron systems. Wave functions for the  $N + 1$  and  $N - 1$  electron systems may be formed by adding or subtracting an orbital from the up- or down-spin determinants of the  $N$ -electron wave function. We call this an "addition/subtraction" calculation. For calculations with periodic boundary conditions the simulation cell is made charge neutral by adding a compensating uniform background charge density. Calculations of this type have been reported for one- [34] and two-dimensional [14] model systems, while results for a three-dimensional system (silicon) are reported in this paper.

QMC calculations of excitation energies in extended systems are computationally very demanding because they are ' $\frac{1}{N}$ ' effects, i.e., the fractional change in energy is inversely proportional to the number of electrons in the system. This means that high statistical accuracy is required to obtain good results. The largest system for which excitation energies have been calculated prior to this paper is 16 atoms (64 electrons). [33] The total finite size error in the ground state energy for that system was estimated to be about 16 eV per simulation cell, while the energy scale of interest for the excitations is of order 0.1 eV. Like almost all methods for calculating excitation energies, QMC calculations of this type only work because of a strong cancellation of errors between the ground and excited states. It turns out that the finite size errors tend to reduce the energy gap, while the errors in the trial wave functions are usually larger for the excited states than for the ground state and so increase the energy gap. Although good agreement with experimental excitation energies has been found using small simulation cells, [31–33] one is left with the suspicion that if larger simulation cells were used the agreement with experiment might be significantly worse because the finite size effects would be smaller. Before these QMC techniques can be relied upon for calculating excitation energies it is necessary that the issue of finite size effects be properly explored. In the next sections we address the following questions:

1. What are the sizes and origins of the finite size effects in excitation energy calculations?
2. What are the differences in finite size effects between promotion and addition/subtraction calculations?

### A. HF theory of excitation energies

First we consider excitation energies for solids within HF theory. The HF equations with the MPC interaction are obtained by minimizing the HF energy of Eq. 16 with respect to the single-particle orbitals, giving

$$\begin{aligned} & -\frac{1}{2}\nabla^2\phi_i + \int \rho(\mathbf{r}')v_E(\mathbf{r}-\mathbf{r}')d\mathbf{r}'\phi_i \\ & - \sum_{i,j}^N \delta_{s_i s_j} \int \phi_j^*(\mathbf{r}')\phi_j(\mathbf{r})\phi_i(\mathbf{r}')f(\mathbf{r}-\mathbf{r}')d\mathbf{r}' \\ & + V_{\text{ext}}\phi_i = \epsilon_i\phi_i \quad . \end{aligned} \quad (19)$$

If we neglect the relaxation of the orbitals, the energy required to excite an electron from the  $j^{\text{th}}$  (occupied) orbital into the  $i^{\text{th}}$  (unoccupied) orbital is

$$\begin{aligned} \Delta E_{ij} = & (\epsilon_i - \epsilon_j) - \int \rho_i(\mathbf{r})\rho_j(\mathbf{r}')v_E(\mathbf{r}-\mathbf{r}')d\mathbf{r}d\mathbf{r}' \\ & + \delta_{s_i s_j} \int \phi_i^*(\mathbf{r})\phi_j^*(\mathbf{r}')\phi_j(\mathbf{r})\phi_i(\mathbf{r}')f(\mathbf{r}-\mathbf{r}')d\mathbf{r}d\mathbf{r}' \\ & + \frac{1}{2} \int \rho_i(\mathbf{r})\rho_i(\mathbf{r}') [v_E(\mathbf{r}-\mathbf{r}') - f(\mathbf{r}-\mathbf{r}')] d\mathbf{r}d\mathbf{r}' \\ & + \frac{1}{2} \int \rho_j(\mathbf{r})\rho_j(\mathbf{r}') [v_E(\mathbf{r}-\mathbf{r}') - f(\mathbf{r}-\mathbf{r}')] d\mathbf{r}d\mathbf{r}' , \end{aligned} \quad (20)$$

where  $\rho_k = |\phi_k|^2$  is the charge density from the  $k^{\text{th}}$  orbital. The first term is the eigenvalue difference for the excitation while the second and third terms are the Hartree and exchange interactions between the electron and hole. Within this approximation the electron-hole terms go to zero in the limit of an infinitely large simulation cell. The fourth and fifth terms on the right hand side are absent if one uses the Ewald interaction instead of the MPC interaction, i.e., we replace  $f$  by  $v_E$ . When the relaxation of the orbitals is neglected these terms also go to zero when the size of the simulation cell goes to infinity because  $v_E$  tends to  $1/r$  over most of the simulation cell.

The addition/subtraction gap is given by

$$\begin{aligned} E_g = & (E_{+i}^{\text{HF}} - E_0^{\text{HF}}) - (E_0^{\text{HF}} - E_{-j}^{\text{HF}}) \\ = & (\epsilon_i - \epsilon_j) \\ & + \frac{1}{2} \int \rho_i(\mathbf{r})\rho_i(\mathbf{r}') [v_E(\mathbf{r}-\mathbf{r}') - f(\mathbf{r}-\mathbf{r}')] d\mathbf{r}d\mathbf{r}' \\ & + \frac{1}{2} \int \rho_j(\mathbf{r})\rho_j(\mathbf{r}') [v_E(\mathbf{r}-\mathbf{r}') - f(\mathbf{r}-\mathbf{r}')] d\mathbf{r}d\mathbf{r}' , \end{aligned} \quad (21)$$

where  $E_0^{\text{HF}}$  is the HF ground state energy of the  $N$ -electron system,  $E_{+i}^{\text{HF}}$  is the energy of the state with an electron added to the  $i^{\text{th}}$  (previously unoccupied) orbital, along with the uniform background charge, and  $E_{-j}^{\text{HF}}$  is the energy of the state where an electron is removed from the  $j^{\text{th}}$  orbital, along with the background charge. The

standard Koopmans' theorem has been modified and contains two additional terms, which also occur in the promotion energy,  $\Delta E_{ij}$ . We have evaluated these additional terms using LDA orbitals and have found that even for a small simulation cell ( $n = 2$ ) they are very small, being in the range  $\pm 0.05$  eV, and they decrease rapidly with system size. We do not expect that the use of exact HF orbitals or orbital relaxation will greatly affect these results.

In Fig. 5 we show the addition/subtraction energies calculated using Eq. 21 for the  $\Gamma_{25'} \rightarrow \Gamma_{15}$  energy gap and the valence band width, calculated with both the Ewald and MPC interactions, along with LDA values. (The results for other energies show similar behaviour.) We do not show the promotion energies in Fig. 5 because they differ from the addition/subtraction energies only by the exciton binding energy, which decreases with increasing system size quite rapidly. Fig. 5 shows that the HF results for the Ewald and MPC interactions are very similar. The band width converges by about  $n = 7$ , but the band gap is still slowly increasing at  $n = 12$ , and the Ewald and MPC values are not yet equal, which they must be at convergence. For the largest system size studied ( $n = 12$ ) the MPC gap and valence band width are 7.4 eV and 17.7 eV respectively, which are a little smaller than the HF values of 8.0 eV and 18.9 eV given in Ref. [35]. Presumably the major reasons for these differences are that we use LDA wave functions and LDA-derived pseudopotentials, although as noted above there is clear evidence that in our calculations the HF energy gap has still not fully converged at  $n = 12$ . The LDA excitation energies converge very rapidly with system size. Note that this would not be true in either LDA or HF theory if we studied isolated clusters of atoms. In a recent study of silicon clusters, Ögüt *et al.* [36] found large differences between the band gap in the LDA eigenvalues and the band gap calculated by electron addition/subtraction. As shown by Franceschetti *et al.* [37], these differences are due to the charging of the cluster when an electron is added or subtracted, which does not occur in our calculations because a uniform background is added to preserve charge neutrality. The slow convergence of the HF excitation energies apparent in Fig. 5 therefore arises from the exchange energy. Moreover, because the results with the Ewald and MPC interactions are almost the same, the source of the error is not the interaction with the exchange hole, but the shape of the exchange hole. This is because the excitation energy depends on the change in the exchange hole due to the excitation, which is not strongly localised.

In a very interesting set of calculations Engel *et al.* [14] studied excited states of a model two-dimensional system using LDA, GW, VMC and DMC techniques. They performed a number of VMC calculations with increasing system size and found that the addition/subtraction gap tended to increase with system size, which is the same

behaviour as we have found in our HF calculations. Engel *et al.* went on to give an explanation of this effect. Their explanation was that in the  $N+1$  ( $N-1$ ) electron systems there is an additional electrostatic energy due to the interaction of the extra electron (hole) with the additional electron (hole) in the other simulation cells. Taking into account the additional compensating uniform background charge that was added to keep each cell neutral, this additional energy is negative and therefore the energies  $E_{N+1}$  and  $E_{N-1}$  are lower than they should be. Engel *et al.* showed that the observed finite size effect is much smaller than the Madelung energy for point charges, and to explain this they argued that the effect would be screened by the response of the other electrons. This argument implies that the finite size effects in addition/subtraction calculations are larger than those in promotion calculations.

Our analysis of the situation is as follows. For simplicity we consider our HF calculations, where the interaction energy can be divided into Hartree and exchange contributions. The significant underestimation of the HF band gaps of small systems is not due to the Hartree terms, which by construction are the same as for our LDA calculations and give very small finite size effects in the band gaps. The finite size error in the HF gaps therefore arises from the exchange energy. By comparing band gaps calculated with the Ewald and MPC interactions we can see whether the problem lies with the interaction or with the shape of the exchange hole. Because we find that the band gaps calculated with the Ewald and MPC interactions are very similar we conclude that the form of the interaction is not the important consideration. Therefore the source of the problem must be the finite size errors present in the shape of the exchange hole. This argument implies that the finite size effects in addition/subtraction calculations are similar to those in promotion calculations. Our viewpoint is supported by the HF results that have been presented in this sub-section and also by the VMC results to be discussed in the next sub-section.

In summary, the HF excitation energies calculated with the Ewald and MPC interactions are very similar. Within HF theory the largest finite size error in excitation energies arises from the shape of the exchange hole, which leads to slow convergence with system size. The finite size errors in promotion and addition/subtraction HF calculations are of similar size.

## B. QMC theory of excitation energies

We now apply the theory developed in the previous section to QMC calculations of excitation energies. Although we have just demonstrated that the HF gaps converge rather slowly with system size, we showed earlier that the finite size effects in VMC and DMC ground state

energies are smaller than in HF theory. It is important to see whether this also applies to excitation energies.

VMC is computationally cheaper than DMC and so we are able to compute excitation energies using VMC over a larger range of system sizes. We expect that the finite size effects in DMC will follow those in VMC, as our VMC calculations retrieve about 90% of the fixed-node correlation energy. We have computed the  $\Gamma_{25'} \rightarrow \Gamma_{15}$  excitation energy in silicon within VMC for the system sizes  $n = 1, 2, 3, 4$  using both promotion and addition/subtraction methods. The calculations were performed with  $\mathbf{k}_s \equiv \Gamma$  and the other computational details were the same as for the ground state calculations. We used Jastrow factors optimized for the ground state of each system which were left unchanged for the excited state. In tests on the  $n = 2$  system we found that separately optimizing the Jastrow factors for both ground and excited states did not significantly change the results. The computational cost of the  $n = 4$  calculations is very large; an error bar in the excitation energies of  $\pm 0.3$  eV requires an error bar of  $\pm 0.0006$  eV per electron. Although the computational effort is large we believe that such a study is necessary to establish the accuracy of QMC excitation energy calculations.

In Fig. 6 we show the excitation energies obtained with the Ewald interaction via the promotion and addition/subtraction methods. (Results for the MPC interaction are very similar.) The promotion and addition/subtraction results are nearly the same, but the promotion energies are slightly smaller because they include an exciton binding energy, which decreases as the system size increases. The results are consistent with a slow increase in the excitation energy with system size and indicate that reasonable convergence is already obtained at  $n = 2$ . The increase in excitation energies with system size is the same trend as in HF calculations, although the finite size errors are smaller in the correlated calculations. The finite size errors in the promotion and addition/subtraction methods are not significantly different at this level of statistical accuracy. On general grounds we expect the finite size effect in the promotion calculation to be slightly larger. This follows because the trend for both promotion and addition/subtraction calculations is that the excitation energy is reduced for small system sizes and this effect is enhanced in the promotion calculation by the exciton binding energy which is larger for small systems. The calculated excitation energy is roughly 4 eV, which is larger than the experimental value of 3.40 eV [38], and also a little larger than our DMC value for an  $n = 2$  simulation cell of 3.7 eV [33]. Our study demonstrates that the largest contribution to the error in the VMC band gap for  $n \geq 2$  arises from the approximate nature of the trial wave functions, and not from finite size effects.

The exciton binding energy can be calculated as the difference between the promotion and addi-

tion/subtraction gaps. The exciton binding energy for the  $\Gamma_{25'} \rightarrow \Gamma_{15}$  excitation is small and we can only resolve it from the statistical noise for the smallest ( $n = 1$ ) cell, which gives a value of  $0.28 \pm 0.01$  eV. In earlier QMC calculations [30–32] the exciton binding energy was estimated using the Mott–Wannier formula

$$E_b \sim \frac{1}{2\epsilon r} , \quad (22)$$

where  $\epsilon$  is the relative permittivity and  $r$  is the radius of the localisation region. Using  $\epsilon = 11.7$  and the appropriate radius for  $n = 1$  of  $r = 4.0$  a.u. gives an exciton binding energy of 0.29 eV. This is extremely close to the VMC value, but the excellent agreement is probably fortuitous since the  $n = 1$  cell is so small that it is appropriate to use a value of  $\epsilon$  at finite wave vector, which would be smaller. The exciton binding energy may also be evaluated within HF theory as the sum of the second and third terms on the r.h.s. of Eq. 20. This gives 0.75 eV for the  $n = 1$  cell using the Ewald interaction, which is considerably larger than the VMC value because the latter calculation includes screening of the electron–electron interaction.

Note that the promotion and addition/subtraction methods differ significantly in the required computational effort. Suppose, for example, that we wish to calculate an energy gap by either the promotion or addition/subtraction methods. Let us assume that the intrinsic variance of the local energy is the same for each of the energies, which is a good approximation for our silicon calculations, and suppose that an acceptable error bar is obtained in a promotion calculation by performing  $M$  Monte Carlo moves for both the ground and excited states. A simple calculation shows that the most efficient way to achieve the same error bar in an addition/subtraction gap is to perform  $2M$  moves for each of the  $N + 1$  and  $N - 1$  systems and  $4M$  for the ground state, giving a total cost of  $8M$  moves. It is therefore four times more expensive to calculate an energy gap to some given accuracy by the addition/subtraction method than by the promotion method.

### C. Modified interaction for excitation energies

In this section we introduce a modified electron–electron interaction specifically designed to describe excitation energies within periodic boundary conditions simulations. Two problems arise when trying to model excitations using finite simulation cells subject to periodic boundary conditions. One is that the excitation is “squeezed” into the simulation cell, and the other is that there are spurious interaction between the periodic replicas of the simulation cell. Here we address the problem of the spurious interactions using the ideas of the MPC

interaction. With our MPC interaction the replicas interact only via the Hartree energy. The charge density on promotion or addition/subtraction of an electron can be written as the sum of the ground state charge density and a small deviation, i.e.,  $\tilde{\rho}(\mathbf{r}) = \rho(\mathbf{r}) + \Delta(\mathbf{r})$ . We can modify the Hartree term so that this charge density interacts with the ground state density in the replicas. This leads to the interaction energy

$$\begin{aligned} \tilde{E}_{e-e} = & \int |\tilde{\phi}|^2 \sum_{i>j} f(\mathbf{r}_i - \mathbf{r}_j) \prod_k d\mathbf{r}_k \\ & + \int \tilde{\rho}(\mathbf{r})\rho(\mathbf{r}') [v_E(\mathbf{r} - \mathbf{r}') - f(\mathbf{r} - \mathbf{r}')] d\mathbf{r} d\mathbf{r}' \\ & - \frac{1}{2} \int \rho(\mathbf{r})\rho(\mathbf{r}') [v_E(\mathbf{r} - \mathbf{r}') - f(\mathbf{r} - \mathbf{r}')] d\mathbf{r} d\mathbf{r}' , \quad (23) \end{aligned}$$

where  $|\tilde{\phi}|^2$  generates the charge density  $\tilde{\rho}$  and the ground state charge density,  $\rho$ , is fixed. A HF analysis of this interaction shows that the HF equations are identical to Eq. 19, so that the orbitals and eigenvalues are unaltered. However, the ground and excited state energy expressions are modified. For the excited states we obtain analogues of Eqs. 20 and 21, but without the terms involving  $(v_E - f)$ , i.e., we retrieve the standard Koopmans’ theorem. We have already shown that these terms are small for silicon, although they will be significant in cases when the change in the charge density due to the excitation is strongly localized. This analysis provides further evidence that the electrostatic interactions between the simulation cell and its replicas is not necessarily an important source of finite size error in excited state energy calculations.

## VIII. CONCLUSIONS

Large Coulomb finite size errors arise in total energy calculations when using the Ewald form of the electron–electron interaction. These finite size errors may be greatly reduced by using our MPC interaction in which the inter-particle interaction is exactly equal to  $1/r$  at short distances and the long range interactions are replaced by a mean-field-like one-electron potential. It is consistent to use the MPC interaction in conjunction with “independent particle finite size corrections” derived from density functional calculations, as long as the latter calculations are performed with the exchange–correlation functional appropriate to the infinite system. Although the long range mean-field-like contribution to the MPC interaction involves the charge density of the system, total energies are insensitive to its form and only an approximate charge density is required.

The MPC interaction can be used consistently for all Coulomb interactions in the system, although it normally reduces to using the MPC interaction for the electron–

electron interaction, retaining the standard Ewald interaction for the electron-ion and ion-ion terms. The Ewald and MPC interactions may be used in tandem as an efficient diagnostic of Coulomb finite size errors. If the Ewald and MPC results agree then the Coulomb finite size error should be small.

If the simulation cell is too small then the confinement of the XC hole makes the XC energy more negative. This source of error is intrinsic to using a finite simulation cell. However, even when the XC hole is artificially confined by a small simulation cell the MPC interaction still gives a better estimate of the XC energy than the Ewald interaction.

Excitation energies calculated within fixed-LDA-orbital HF theory show significant finite size effects. However, in correlated calculations the finite size effects are smaller and accurate excitation energies can be obtained using quite small simulation cells. In silicon we find that the finite size errors in VMC electron-promotion (“optical absorption”) and electron addition/subtraction (“photoemission”) calculations are similar, and that the optical promotion method has the greater statistical efficiency. The finite size errors for low lying excitations in silicon are small, and quite accurate results may be obtained from 16 atom cells.

We have described new developments aimed at understanding and reducing finite size errors in many-body quantum simulations using periodic boundary conditions. Since one cannot get exact answers for an infinite system from a finite simulation cell whatever interaction is used, there is no “exact interaction” for a finite system with periodic boundary conditions. The Ewald and MPC interactions are alternative model interactions compatible with periodic boundary conditions, and the relevant question is which model interaction gives results which most closely approximate those for very large simulation cells. The Ewald and MPC interactions differ by an amount which is inversely proportional to the size of the simulation cell and therefore they give the same energy per particle in the limit of an infinitely large simulation cell. However, for finite cells the Ewald and MPC interactions can give significantly different energies. In every test we have performed the energy calculated with the MPC interaction is closer than the Ewald energy to the value for a very large system. The MPC interaction is applicable to both metals and insulators and it is faster to compute than the Ewald interaction. Given these facts we believe that the MPC interaction should be used for all quantum many-body calculations of total energies in systems with periodic boundary conditions.

## IX. ACKNOWLEDGMENTS

Financial support was provided by the Engineering and Physical Sciences Research Council (UK). Our calculations

are performed on the CRAY-T3E at the Edinburgh Parallel Computing Centre and the Hitachi SR2201 located at the University of Cambridge High Performance Computing Facility.

- 
- \* Present address: National Renewable Energy Laboratory, Golden, Colorado 80401, USA.
- [1] W. L. McMillan, Phys. Rev. **138**, A442 (1965); D. Ceperley, G. V. Chester, and M. H. Kalos, Phys. Rev. B **16**, 3081 (1977).
  - [2] D. M. Ceperley and M. H. Kalos, in *Monte Carlo Methods in Statistical Physics*, edited by K. Binder (Springer, Berlin 1979); K. E. Schmidt and M. H. Kalos, in *Monte Carlo Methods in Statistical Physics II*, edited K. Binder (Springer, Berlin 1984).
  - [3] B. L. Hammond, W. A. Lester, Jr., and P. J. Reynolds, *Monte Carlo Methods in ab initio quantum Chemistry*, (World Scientific, Singapore, 1994).
  - [4] All equations are given in Hartree atomic units ( $\hbar = m_e = e = 4\pi\epsilon_0 = 1$ ).
  - [5] S. W. de Leeuw, J. W. Perram, and E. R. Smith, Proc. Roy. Soc. Lond. A **373**, 27 (1980).
  - [6] P. P. Ewald, Ann. Phys. (Leipzig) **64**, 253 (1921).
  - [7] The reduction of the problem to one within the primitive unit cell is only possible within independent particle theories; in a true many-body theory one has to solve over the entire simulation cell.
  - [8] J. P. Perdew and A. Zunger, Phys. Rev. B **23**, 5048 (1981).
  - [9] D. M. Ceperley and B. J. Alder, Phys. Rev. Lett. **45**, 566 (1980).
  - [10] D. M. Ceperley, Phys. Rev. B **18**, 3126 (1978).
  - [11] D. M. Ceperley and B. J. Alder, Phys. Rev. B **36**, 2092 (1987).
  - [12] B. Tanatar and D. M. Ceperley, Phys. Rev. B **39**, 5005 (1989).
  - [13] Y. Kwon, D. M. Ceperley and R. M. Martin, unpublished.
  - [14] G. E. Engel, Y. Kwon, and R. M. Martin, Phys. Rev. B **51**, 13538 (1995).
  - [15] L. M. Fraser, W. M. C. Foulkes, G. Rajagopal, R. J. Needs, S. D. Kenny, and A. J. Williamson, Phys. Rev. B **53**, 1814 (1996).
  - [16] A. J. Williamson, G. Rajagopal, R. J. Needs, L. M. Fraser, W. M. C. Foulkes, Y. Wang, and M.-Y. Chou, Phys. Rev. B **55**, R4851 (1997).
  - [17] A. Baldereschi, Phys. Rev. B **7**, 5212 (1973).
  - [18] H. J. Monkhorst and J. D. Pack, Phys. Rev. B **13**, 5188 (1976).
  - [19] G. Rajagopal, R. J. Needs, S. Kenny, W. M. C. Foulkes, and A. James, Phys. Rev. Lett. **73**, 1959 (1994).
  - [20] G. Rajagopal, R. J. Needs, A. James, S. Kenny, and W. M. C. Foulkes, Phys. Rev. B **51**, 10591 (1995).
  - [21] See, for example, C. Kittel, *Introduction to Solid State Physics*, 7th edition (Wiley, New York, 1996).

- [22] A. J. Williamson, S. D. Kenny, G. Rajagopal, A. J. James, R. J. Needs, L. M. Fraser, W. M. C. Foulkes, and P. Maccallum, Phys. Rev. B **53**, 9640 (1996).
- [23] C. J. Umrigar, K. G. Wilson, and J. W. Wilkins, Phys. Rev. Lett. **60**, 1719, (1988).
- [24] S. Fahy, X. W. Wang, and S. G. Louie, Phys. Rev. B **42**, 3503 (1990).
- [25] M. M. Hurley and P. A. Christiansen, J. Chem. Phys. **86**, 1069, 1987; B. L. Hammond, P. J. Reynolds, and W. A. Lester, Jr., *ibid.* **87**, 1130, 1987, L. Mitáš, E. L. Shirley, and D. M. Ceperley, *ibid.*, **95**, 3467, (1991).
- [26] X. P. Li, D. Ceperley, and R. M. Martin, Phys. Rev. B **44**, 10929 (1991).
- [27] O. W. Day, D. W. Smith, and C. Garrod, Int. J. Quantum Chem. Symp. **8**, 501 (1974).
- [28] M. M. Morrell, R. G. Parr, and M. Levy, J. Chem. Phys. **62**, 549 (1975).
- [29] P. R. C. Kent, Randolph Q. Hood, M. D. Towler, R. J. Needs, and G. Rajagopal. Phys. Rev. B. **57**, 15293 (1998).
- [30] L. Mitáš and R. M. Martin, Phys. Rev. Lett. **72**, 2438, (1994).
- [31] L. Mitáš, Comput. Phys. Commun. **96**, 107, (1996).
- [32] L. Mitáš, *Electronic Properties of Solids Using Cluster Methods*, eds. T. A. Kaplan and S. D. Mahanti (Plenum, New York, 1995), p151.
- [33] A. J. Williamson, R. Q. Hood, R. J. Needs, and G. Rajagopal. Phys. Rev. B. **57**, 12140 (1998).
- [34] W. Knorr and R. W. Godby, Phys. Rev. Lett. **68**, 639, (1992).
- [35] W. von der Linden and P. Horsch, quoted in W. Borrmann and P. Fulde, Phys. Rev. B **35**, 9569, (1987).
- [36] S. Ögüt, J. R. Chelikowsky and S. G. Louie, Phys. Rev. Lett. **79**, 1770, (1997).
- [37] A. Franceschetti, L.-W. Wang and A. Zunger, unpublished.
- [38] *Numerical Data and Functional Relationships in Science and Technology*, edited by K.-H. Hellwege and O. Madelung, Landolt-Börnstein, New Series, Group III, Vol. 17a (Springer, Berlin, 1982).

FIG. 1. Convergence of the LDA and HF ground state energies per atom of silicon as a function of simulation cell size,  $n$ , using  $\Gamma$ -point BZ sampling.

FIG. 2. The LDA and HF ground state energies per atom of silicon as a function of simulation cell size,  $n$ , using  $L$ -point BZ sampling.

FIG. 3. The VMC ground state energies per atom of silicon as a function of simulation cell size,  $n$ . A correction for the IPFSE is included. The statistical error bars are  $\pm 0.01$  eV per atom.

FIG. 4. The DMC ground state energies per atom of silicon as a function of simulation cell size,  $n$ . A correction for the IPFSE is included. The statistical error bars are  $\pm 0.02$  eV per atom.

FIG. 5. Convergence of the  $\Gamma_{25'} \rightarrow \Gamma_{15}$  excitation energy and valence band width of silicon. The data correspond to addition/subtraction energies calculated within HF theory as a function of simulation cell size,  $n$ , using both the MPC and Ewald interactions. LDA results are also shown.

FIG. 6. The  $\Gamma_{25'} \rightarrow \Gamma_{15}$  excitation energy of silicon calculated within VMC theory as a function of simulation cell size,  $n$ . Data for the Ewald interaction are shown obtained via both the promotion and addition/subtraction methods.

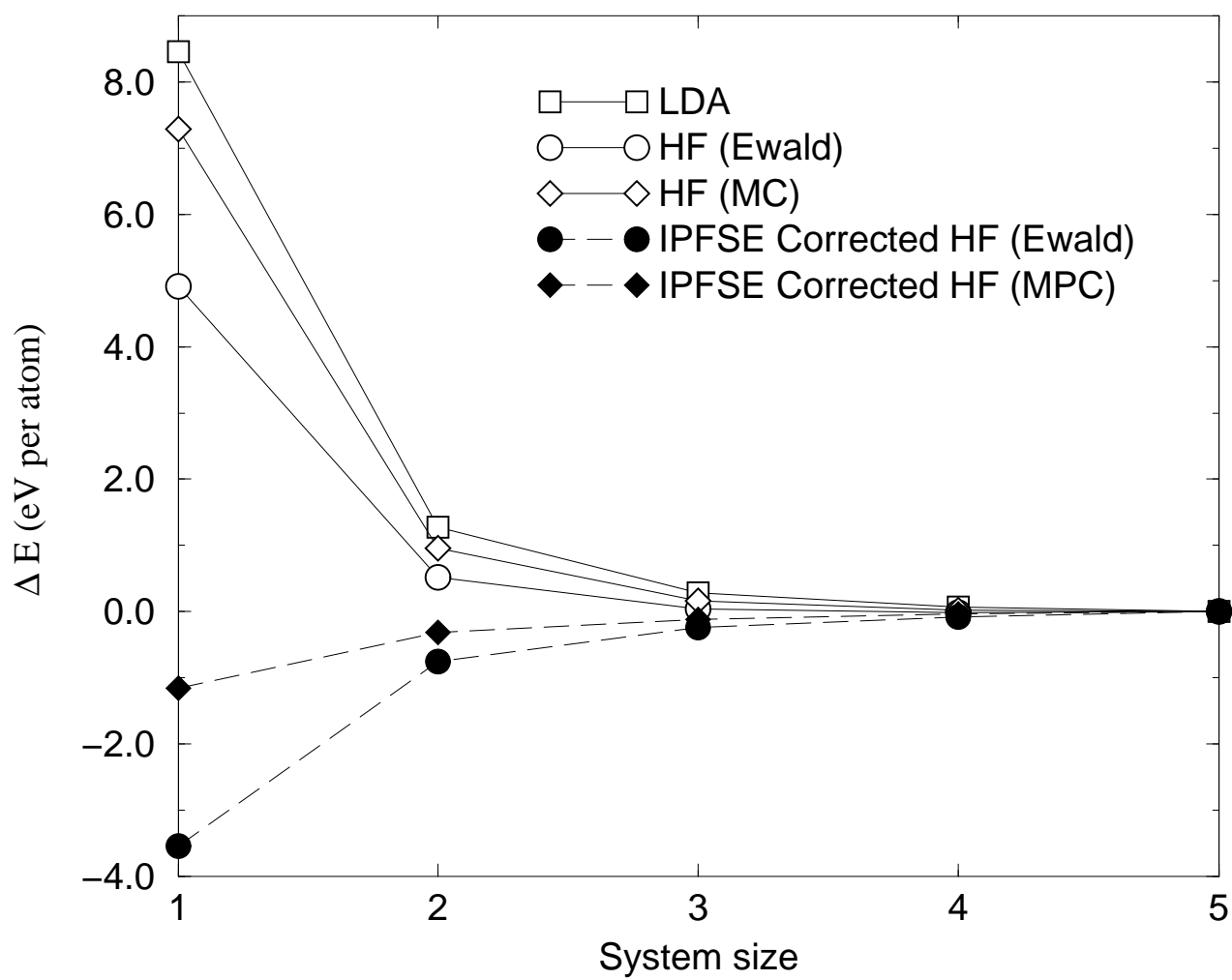


Figure 1 Kent et. al.



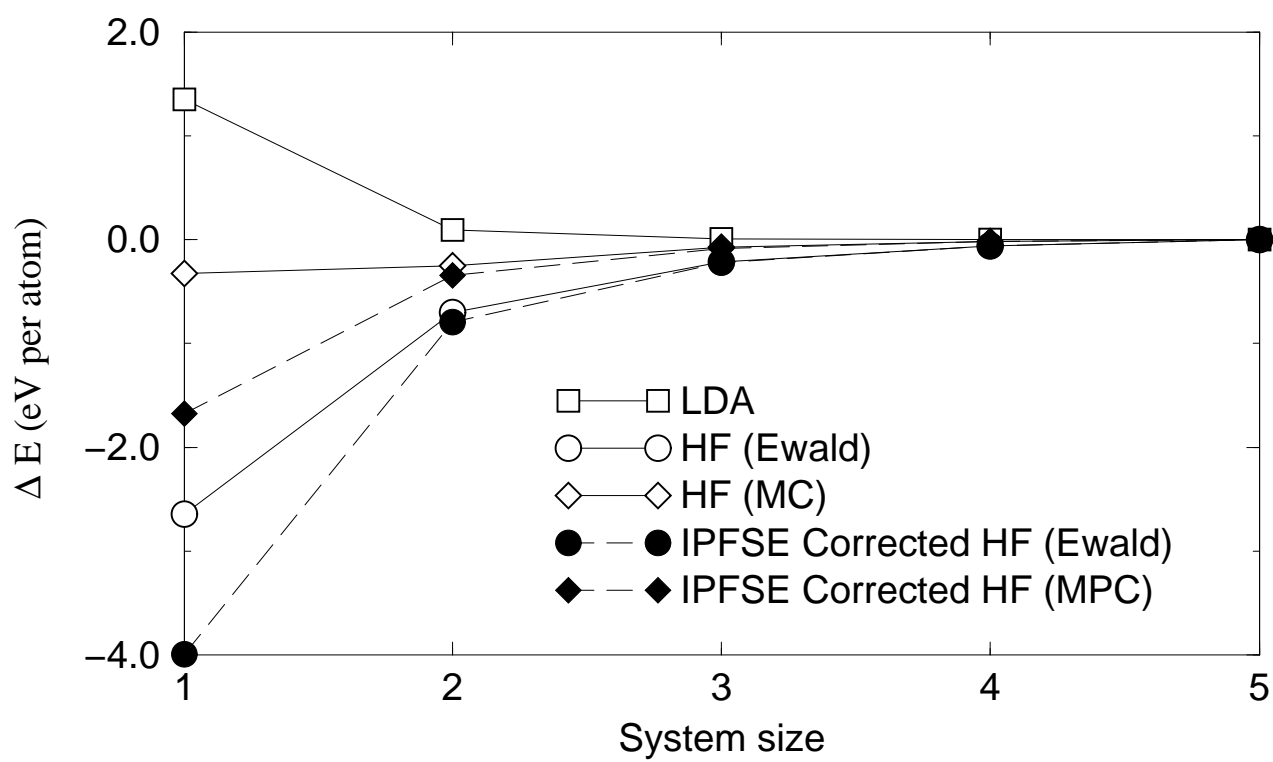


Figure 2 Kent et. al.

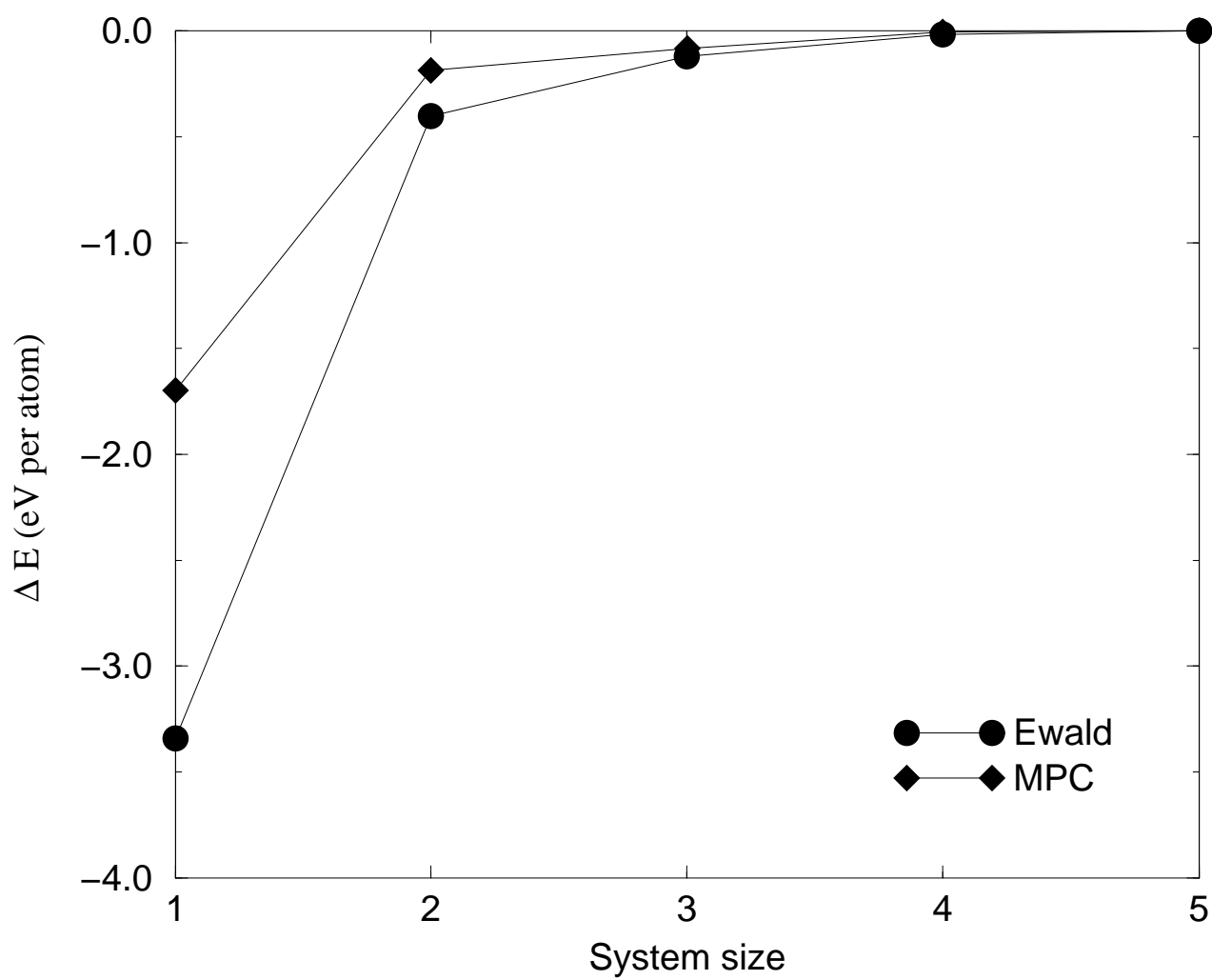


Figure 3 Kent et. al.

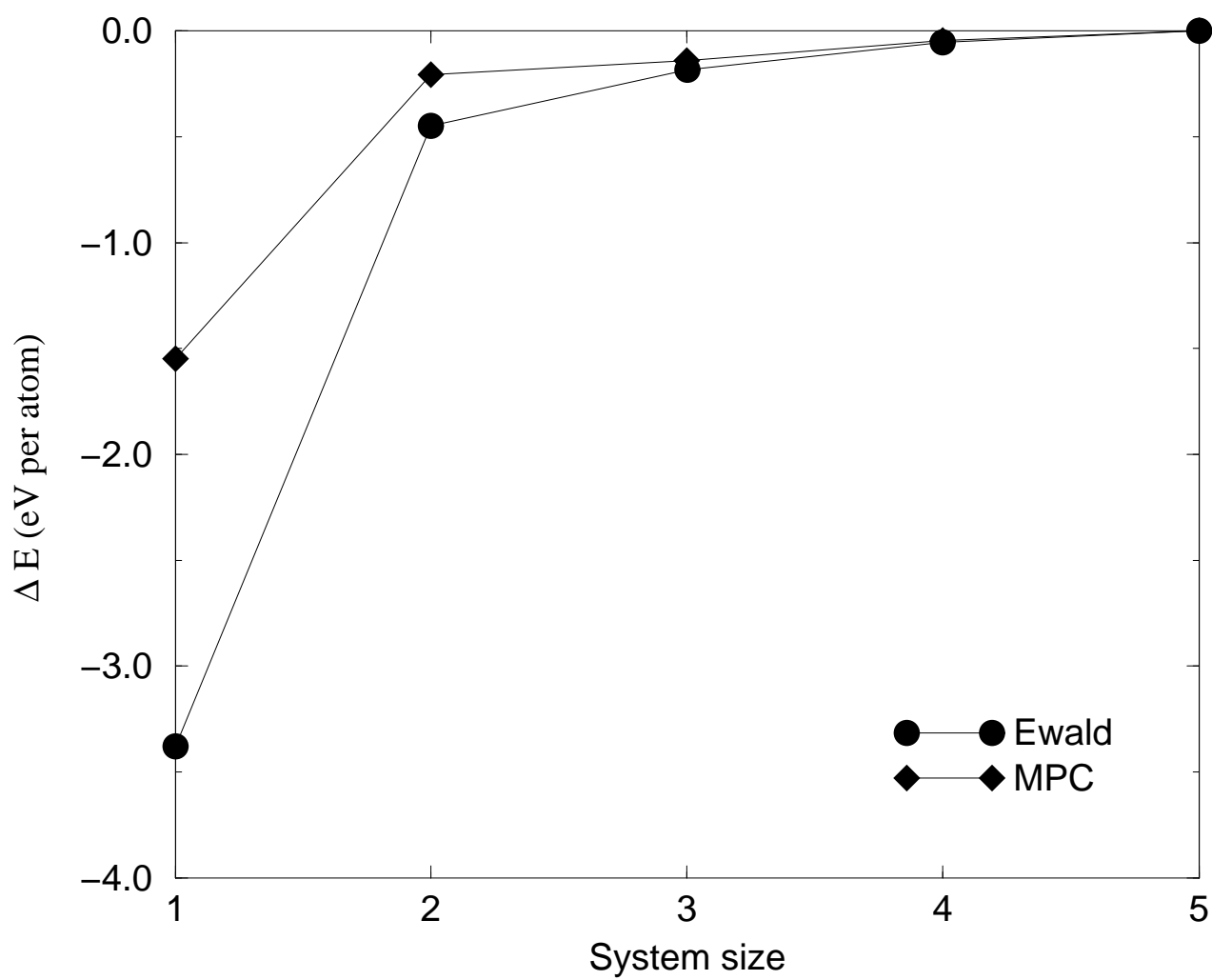


Figure 4 Kent et. al.

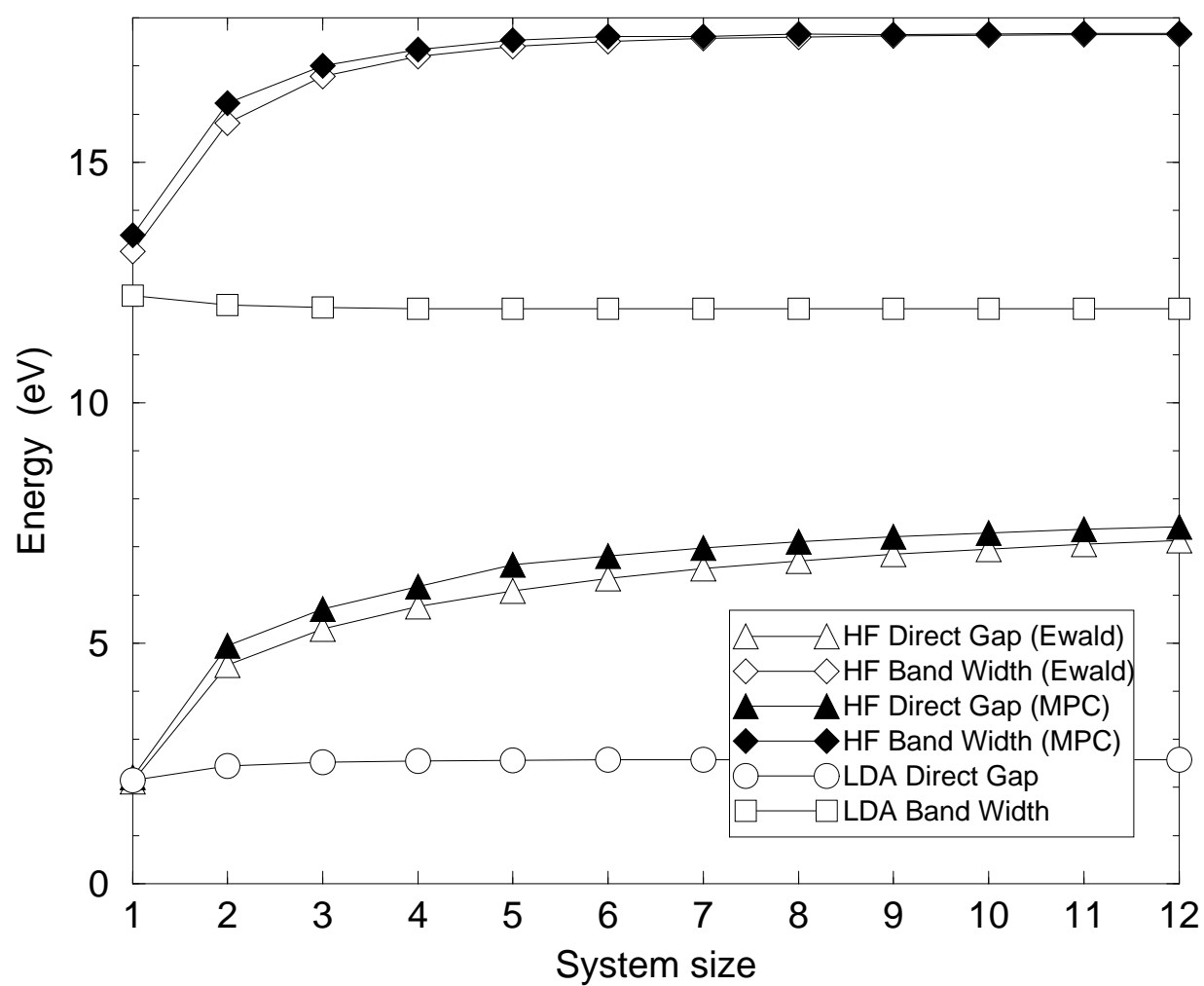


Figure 5 Kent et. al.

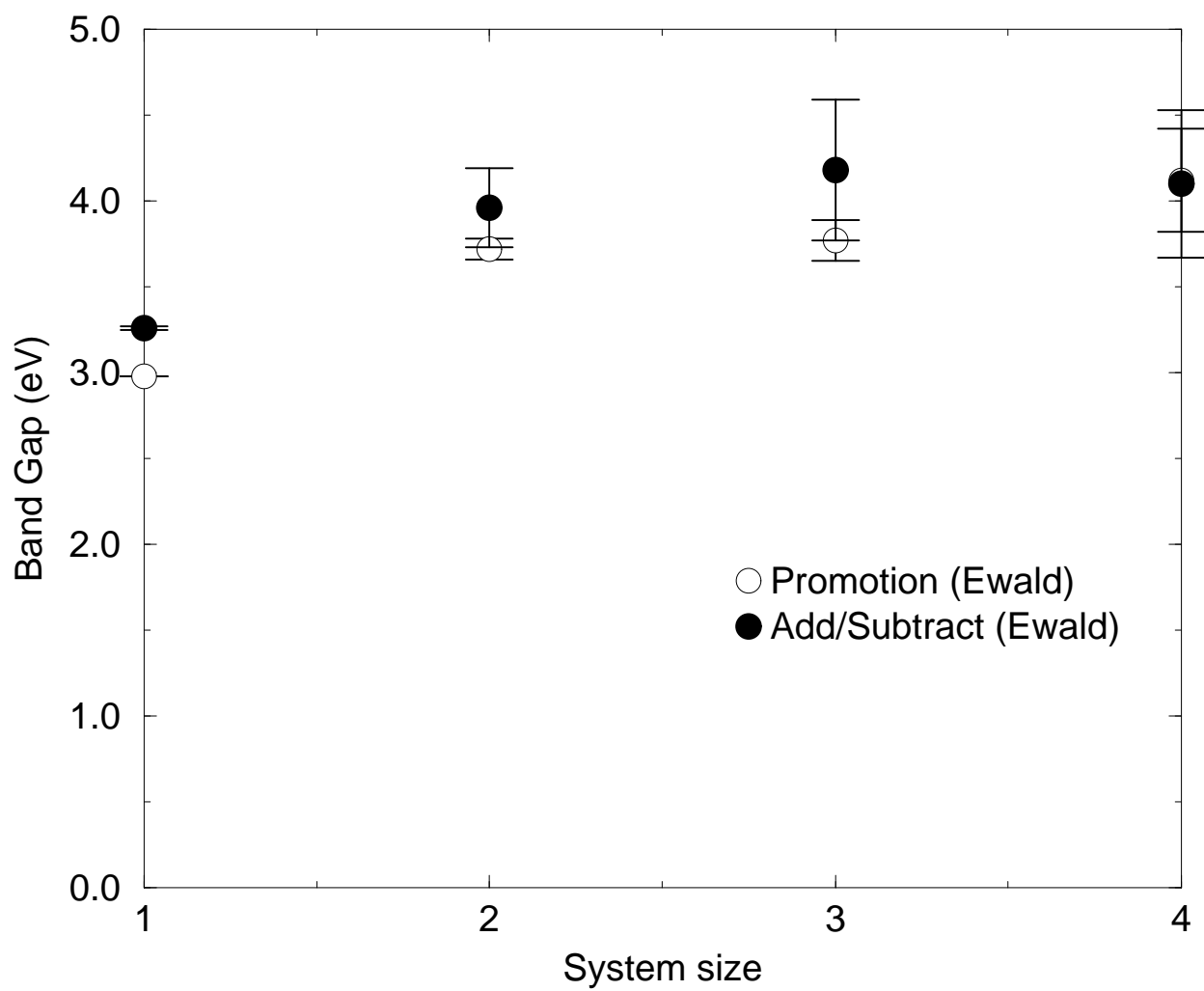


Figure 6 Kent et. al.